

# Hierarchical Relation-augmented Representation Generalization for Few-shot Action Recognition

Hongyu Qu  
Nanjing University of Science and  
Technology  
quhongyu@njjust.edu.cn

Ling Xing  
Nanjing University of Science and  
Technology  
lingxing@njjust.edu.cn

Rui Yan  
Nanjing University of Science and  
Technology  
ruiyan@njjust.edu.cn

Yazhou Yao  
Nanjing University of Science and  
Technology  
yazhou.yao@njjust.edu.cn

Guo-Sen Xie  
Nanjing University of Science and  
Technology  
gsxiehm@gmail.com

Xiangbo Shu\*  
Nanjing University of Science and  
Technology  
shuxb@njjust.edu.cn

## ABSTRACT

Few-shot action recognition (FSAR) aims to recognize novel action categories with few exemplars. Existing methods typically learn frame-level representations independently for each video by designing various inter-frame temporal modeling strategies. However, they neglect explicit relation modeling between videos and tasks, thus failing to capture shared temporal patterns across videos and reuse temporal knowledge from historical tasks. In light of this, we propose HR<sup>2</sup>G-shot, a Hierarchical Relation-augmented Representation Generalization framework for FSAR, which unifies three types of relation modeling (inter-frame, inter-video, and inter-task) to learn task-specific temporal patterns from a holistic view. In addition to conducting inter-frame temporal interactions, we further devise two components to respectively explore inter-video and inter-task relationships: **i)** Inter-video Semantic Correlation (ISC) performs cross-video frame-level interactions in a fine-grained manner, thereby capturing task-specific query features and learning intra- and inter-class temporal correlations among support features; **ii)** Inter-task Knowledge Transfer (IKT) retrieves and aggregates relevant temporal knowledge from the bank, which stores diverse temporal patterns from historical tasks. Extensive experiments on five benchmarks show that HR<sup>2</sup>G-shot outperforms current top-leading FSAR methods. Full code will be released.

## 1 INTRODUCTION

During the last few years, action recognition [4, 11, 15, 16, 23, 42, 58] has witnessed remarkable progress with the advances in deep learning. However, their strong performance heavily relies on a large amount of labeled training examples, which restricts the model’s scalability and generalizability in data scarcity scenarios. In contrast, human beings can easily learn new visual concepts with only a few supervisions. To enable the machine to acquire such ability, many studies have shifted their attention towards few-shot action recognition (FSAR) [3, 48, 69], which aims to learn novel (unseen) action classes using only a few annotated video samples after training on a set of base (seen) classes with abundant samples.

Current top-leading FSAR solutions typically adopt the metric-based meta-learning paradigm, wherein the model first maps the query videos and support videos into discriminative feature space,

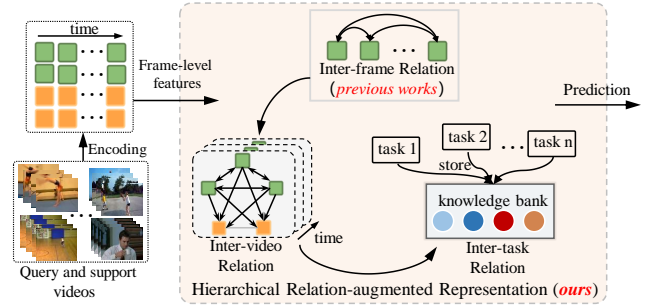


**Figure 1: Our main idea. Previous FSAR works only rely on inter-frame relation modeling to learn video representations, ignoring the relations between videos and tasks. In contrast, we unify three types of relation modeling (i.e., inter-frame, inter-video, inter-task) under one single framework, so as to capture task-specific temporal cues.**

and then performs query-support video matching based on predefined or learned distance metrics. To achieve this, a prevalent of subsequent efforts delve into network designs for **temporal representation learning** by, e.g., temporal attention operations [47], elaborated spatio-temporal [40] or temporal-channel interaction [57], multi-layer feature fusion [56], and auxiliary modal information (e.g., depth [13] and motion [46]). Apart from investigating **temporal representation learning**, to perform proper temporal feature alignment when comparing query and support videos, recent approaches devise **various temporal matching strategies**, e.g., frame-level feature matching [3, 48], tuple-level feature matching [28], frame-to-segment feature matching [52], or multi-level feature matching [66].

Though achieving remarkable performance, these methods suffer from two limitations: **First**, they independently learn frame-level representations for each video, **neglecting the relation modeling and holistic semantic patterns among video samples in the current task**. Exploring inter-video relationships can not only learn subtle semantic discrepancies among different videos, but also capture shared similar temporal patterns (e.g., action styles and speed) from diverse video samples, particularly under data-limited conditions. Although some preliminary attempts [47, 57] have been made towards this, they capture sample-level correlations at the video level (global feature for each video), ignoring fine-grained temporal details in videos. Thus, these methods fail to capture shared temporal patterns across videos in each task. **Second**, exist-

\*Corresponding author.

ing methods directly learn meaningful video representation from one single task, *lacking explicit modeling of task-relatedness* (i.e., some tasks share similar action patterns or structures). Thus, they fail to reuse experience from historical tasks and excavate task-shared temporal knowledge, causing sub-optimal transferability and generalization on new tasks with only a few samples. In light of the above, our goal is to *unify three types of relation modeling (i.e., inter-frame, inter-video, inter-task) under one single framework*, so as to yield task-specific temporal features for each video via transferring knowledge at both video-level and task-level (as shown in Fig. 1).

In this vein, we develop a novel hierarchical framework for FSAR, namely HR<sup>2</sup>G-shot, which learns task-specific temporal cues from multiple perspectives (i.e., inter-frame, inter-video, inter-task) in a progressive manner. In addition to performing inter-frame temporal interactions, we further explicitly learn inter-video and inter-task relationships, so as to strengthen temporal pattern understanding for each video from a holistic view. Thus, we propose two feasible modules: **i) Inter-video Semantic Correlation (ISC)** aims to precisely capture inter-video temporal relationships within each task. Specifically, we perform cross-video frame-level interactions in a fine-grained manner to gain task-specific temporal features and reduce considerable computational costs compared with inter-video dense interaction (see Table 3). Moreover, to respect the difference between support and query videos, we customize the masked interaction strategy for support-support and query-support relations (i.e., support and query videos only aggregate semantic information from support videos). By this means, our model could interactively transfer temporal knowledge between videos to yield task-specific query features and learn intra- and inter-class correlation among support features. **ii) Inter-task Knowledge Transfer (IKT)** is devised to learn transferable temporal knowledge between tasks by exploring inter-task relationships. Concretely, we develop a temporal knowledge bank to store diverse temporal patterns from historical tasks. Then we make use of temporal prototypes, which summarize frame-level representations of each video, to retrieve and aggregate temporal knowledge related to new tasks from the bank. Integrated with such knowledge, our method yields more meaningful video representations, thus quickly adapting to new tasks with only a few samples. We conduct extensive experiments on five gold-standard datasets, and the results demonstrate that our HR<sup>2</sup>G-shot outperforms existing top-leading FSAR methods by a large margin.

Overall, the main contributions of this work are threefold:

- We provide a hierarchical relation-augmented framework for FSAR, which unifies three types of relation modeling to learn task-specific temporal patterns.
- **To explore inter-video temporal relationships within each task**, we propose Inter-video Semantic Correlation that conducts cross-video frame-level interactions in a fine-grained manner and customizes masked interaction strategy for support-support and query-support relations.
- **To learn transferable temporal knowledge between tasks**, we design Inter-task Knowledge Transfer that retrieves and aggregates relevant temporal knowledge from

the temporal knowledge bank, which stores diverse temporal patterns from historical tasks.

## 2 RELATED WORK

**Few-shot Image Classification.** The goal of few-shot image classification [10] is to recognize unseen categories with limited annotated samples. Existing few-shot solutions can be broadly categorized into three groups: **i) Augmentation-based** methods typically generate auxiliary data samples by feature augmentation [1, 7, 8] or generative models [24, 64], to increase the diversity of the support set; **ii) Optimization-based** methods [12, 20, 32, 33, 36] learn good initial model parameters, such that updating the initial parameters via a few gradient steps could adapt well to new tasks; **iii) Metric-based** methods [9, 60, 61, 68] (e.g., ProtoNet [34] and RelationNet [37]) first learn a common feature space for all classes, and then employ pre-defined or learned distance metrics to compare query and support samples.

Our work shares a similar spirit of metric-based methods [34, 41], whereas we address more complex and challenging few-shot action recognition that requires long-range relation modeling between spatio-temporal locations. With respect to this, we further jointly learn inter-video and inter-task relationships to learn distinct temporal features. By unifying such three types of relation modeling under our framework, we can learn task-specific temporal cues for each video from a holistic view.

**Few-shot Action Recognition (FSAR).** FSAR is gaining much attention due to its practical value in reducing manual annotations at a large scale required by traditional action recognition. Compared with few-shot image classification, FSAR is more challenging due to the rich spatial-temporal information in videos. Towards FSAR, most existing solutions [27, 38, 43, 51] belong to the meta-learning paradigm [34, 41], wherein the model learns discriminative temporal features from base action categories, and generalizes learned temporal representations on novel action categories. Based on the meta-learning policy, a main group of efforts focus on *temporal representation learning*. Early works [69, 70] directly aggregate frame-level features to learn a global representation for each video. Though straightforward, these methods neglect complex temporal cues within one video, leading to suboptimal performance. To address this limitation, recent methods attempt to model temporal relations by, e.g., learning long-range temporal dependencies [40, 47], detailed cross-frame patch-level interactions [65], exploiting low-level spatial features via feature architecture search [56], or multi-modal feature fusion [13, 17, 44, 50]. Apart from investigating video feature representation, another line of work turns to designing various *feature matching strategies*, e.g., frame-level feature alignment [47], tuple-level feature alignment [28], and even multi-level feature alignment [18, 51, 66]. For example, OTAM [3] performs frame-level feature alignment between videos with the DTW algorithm, which takes the temporal ordering characteristics of videos into account. HyRSM [47] designs a novel bidirectional Mean Hausdorff metric to obtain temporal matching scores between support and query videos from the set matching perspective.

Despite promising results have been achieved, they typically learn temporal representations independently for each video, ignoring the relation modeling between video samples and tasks. As

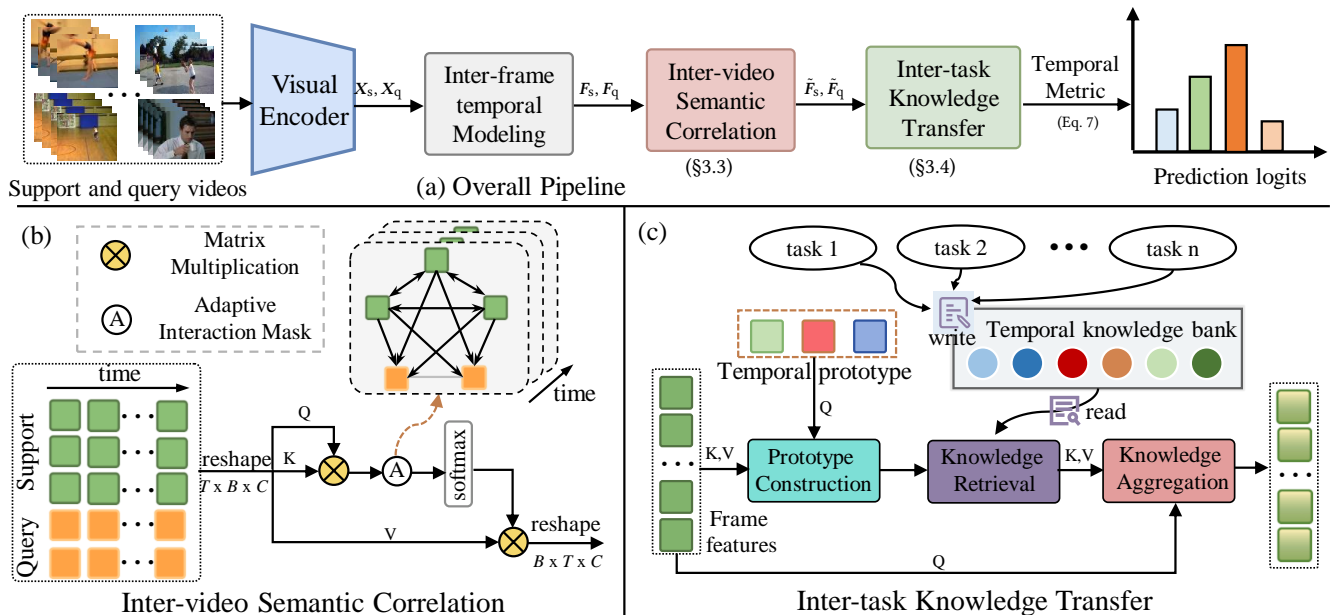


**Figure 2: The overview of HR<sup>2</sup>G-shot. (a) HR<sup>2</sup>G-shot unifies three types of relation modeling (*i.e.*, inter-frame, inter-video, and inter-task) to learn discriminative temporal features. (b) Inter-video Semantic Correlation (ISC) conducts fine-grained cross-video interactions to learn inter-video relationships. (c) To explore inter-task relationships, we retrieve and aggregate temporal knowledge from the bank, which maintains diverse temporal patterns from historical tasks.**

a result, they fail to gain a holistic semantic pattern understanding from multi-level perspectives. Though a few works (*e.g.*, GgHM [57] and HyRSM [47]) attempt to learn task-specific embeddings by considering inter-task relationships, they only focus on the correlations between samples at the video level, overlooking fine-grained temporal interactions among videos. In contrast, our HR<sup>2</sup>G-shot **i)** learns inter-video relationships at fine-grained frame level, and **ii)** gather temporal knowledge from historical tasks to achieve inter-task knowledge transfer, thereby capturing task-specific temporal features for each video and ensuring a sufficient understanding of holistic semantic patterns for each task.

## 3 METHOD

### 3.1 Problem Formulation

The objective of few-shot action recognition (FSAR) is to classify novel action categories with limited samples per class. Under the few-shot setting, the model generalizes learned knowledge on training set  $\mathcal{D}_{base}$  to novel testing set  $\mathcal{D}_{novel}$ , where base classes  $C_{base}$  and novel classes  $C_{novel}$  are disjoint. Consistent with previous works [3, 39, 47], we formulate FSAR problem with episodic training and testing. Specifically, each  $N$ -way  $K$ -shot episode task involves sampled  $K$  labeled videos from each of  $N$  different action classes as the support set, and a portion of the remaining samples from  $N$  classes as the query set. During inference, we randomly sample multiple episodic tasks from  $\mathcal{D}_{novel}$  and present the average results over these tasks, in order to comprehensively evaluate the performance of the few-shot model.

### 3.2 Algorithm Overview

We introduce HR<sup>2</sup>G-shot, which hierarchically models multi-level relations (*i.e.*, inter-frame, inter-video, and inter-task) to capture task-specific temporal patterns from a holistic view for FSAR. The overall architecture of HR<sup>2</sup>G-shot is shown in Fig. 2. Given an  $N$ -way  $K$ -shot episode task with  $NK$  support videos and  $L$  query videos, we employ CLIP visual encoder [31] to get frame-level features for support and query videos, *i.e.*,  $X_s \in \mathbb{R}^{NK \times T \times C}$  and  $X_q \in \mathbb{R}^{L \times T \times C}$ , where  $T$  is the length of sampled frames in each video. Note that we adopt Parameter-Efficient Fine-Tuning (PEFT) strategy to fine-tune the visual encoder with minimal trainable parameters as in [29, 55, 59]. Next, following previous works [45], we concatenate frame-level features and corresponding textual features along the temporal dimension and then feed into temporal Transformer [45, 46] (*i.e.*, Inter-frame Temporal Modeling). In this way, we perform inter-frame interactions and obtain enhanced support and query features. To compensate frame-level relation modeling from other semantic perspectives, we further design two feasible modules: **i)** Inter-video Semantic Correlation (ISC) (§3.3) learns inter-video temporal relationships within each task by fine-grained cross-video interactions; **ii)** Inter-task Knowledge Transfer (IKT) (§3.4) aggregates useful temporal knowledge from historical tasks to learn inter-task relationships. Finally, the obtained task-specific support and query features, *i.e.*,  $\bar{F}_s$  and  $\bar{F}_q$ , are fed into temporal matching metrics to get the class predictions.

### 3.3 Inter-video Semantic Correlation

Different from exploiting inter-frame interactions in each video, capturing inter-video relationships can strengthen task-specific

semantic patterns for each video. To achieve this goal, we design Inter-video Semantic Correlation (ISC) module to conduct **Fine-grained Inter-video Interaction** and further learn intra- and inter-class correlation by **Adaptive Interaction Mask** (Fig. 3(a)) for support-query and support-support videos (Fig. 2(b)). Via Adaptive Interaction Mask, support and query videos aggregate features from different types of videos (*i.e.*, support or query) based on their respective characteristics. Compared with previous works [47, 57], which only consider utilize global video features to perform interactions among support and query videos, we attempt to make use of temporal cues in the video to strengthen sufficient temporal pattern understanding among videos.

**Fine-grained Inter-video Interaction.** Based on the above analysis, how to perform fine-grained inter-video interactions is crucial for FSAR. A straightforward approach is to perform dense attention along temporal and sample dimensions simultaneously. Thus, given a task with  $NK$  support videos and  $L$  query videos, the computational complexity of such dense sample attention is  $O((NK+L)^2T^2)$ , causing high computational costs. Besides, due to the difference between the temporal dimension and the sample dimension, it is not reasonable to treat them equivalently.

Thus, we decouple dense sample attention into inter-frame interaction and our designed Inter-video Semantic Correlation (ISC). The inter-frame interaction is achieved by previous Inter-frame Temporal Modeling, obtaining support and query temporal features, *i.e.*,  $F_s \in \mathbb{R}^{NK \times T \times C}$  and  $F_q \in \mathbb{R}^{L \times T \times C}$ . Next, ISC concatenates support and query features, and reshapes these features in one task to  $\mathbb{R}^{T \times (NK+L) \times C}$ . Afterwards, multi-head self-attention along with sample attention matrix  $A \in \mathbb{R}^{(NK+L) \times (NK+L)}$  is adopted to conduct cross-video interactions by attending all frame features at the same temporal location, resulting in task-specific temporal futures for support and query videos:

$$\tilde{F} = [\tilde{F}_s, \tilde{F}_q] = \text{SelfAttn}(\text{Re}(\text{Cat}(F_s, F_q))), \quad (1)$$

where  $\text{Re}$  is the reshape operation, and  $\text{Cat}$  denotes the concatenation operation.  $\text{SelfAttn}$  represents the standard multi-head self-attention. As such, ISC not only captures task-specific temporal features via interactively transfer temporal knowledge between videos, but also reduces the computational complexity to  $O((NK+L)^2T)$  (see Table 3).

**Adaptive Interaction Mask.** Due to the difference between support and query videos, we propose Adaptive Interaction Mask  $J \in \mathbb{R}^{(NK+L) \times (NK+L)}$  for support-support and query-support interactions, as shown in Fig. 3(a). Specifically in each task, support and query videos only aggregate semantic information from support videos while discarding interactions with query videos by element-wise multiplication of  $A$  and  $J$ . By transferring knowledge between support-support and query-support videos, support features could learn intra- and inter-class correlation, and query features capture task-specific temporal cues. Besides, as shown in Fig. 3(b)(c)(d), we try other masked interaction strategies for inter-video interactions, including *support-support interaction*, *query-support interaction* and *full interaction*. Specifically, *support-support interaction* denotes ISC only considers the interactions among support videos, while *query-support interaction* denotes query videos only aggregate semantic information from support videos in ISC. *full interaction* means ISC

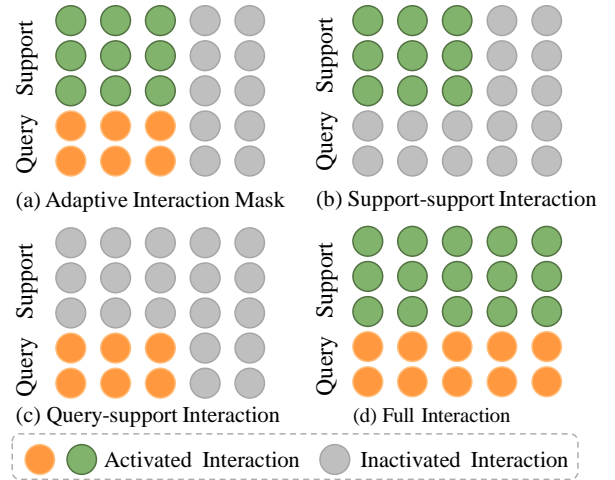


**Figure 3: Different masked interaction strategies for Inter-video Semantic Correlation.**

simultaneously considers the interactions among query and support videos, but ignores the distinct characteristics of the query and support videos. The experiments about different strategies are provided in Table 4a.

### 3.4 Inter-task Knowledge Transfer

Previous FSAR methods typically learn video representations within a single task, failing to explicitly learn transferable temporal knowledge between tasks. Thus, these methods lack generalizability and transferability on unseen action categories. To compensate for this limitation, we design Inter-task Knowledge Transfer (IKT) module to aggregate useful temporal knowledge from the bank, which stores diverse temporal cues shared by different tasks. IKT consists of prototype construction, knowledge retrieval, knowledge aggregation and knowledge bank updating, as shown in Fig. 2(c).

**Prototype Construction.** The core idea is to incorporate frame-level features into compact temporal prototypes, so as to filter out redundant information and obtain key temporal cues. We first construct  $M$  learnable prototypes  $P \in \mathbb{R}^{M \times C}$  to summarize video representations, where we empirically set  $M$  to 3 (ablation study in Table 4c). Given a task consisting of support and query videos, these prototypes adaptively aggregate action dynamic information from support features  $\tilde{F}_s \in \mathbb{R}^{NK \times T \times C}$ :

$$\hat{P} = \text{Softmax}(PK_t^T)V_t + P, \quad (2)$$

where  $K_t$  and  $V_t$  are the linear transformation features of frame-level features  $\tilde{F}_s$ . As such, such prototypes  $\hat{P}$  can adaptively learn useful temporal patterns.

**Knowledge Retrieval.** Inspired by [53, 67], we setup a temporal knowledge bank  $M = [m_1, m_2, \dots, m_G] \in \mathbb{R}^{G \times C}$  to store task-shared temporal patterns, where  $G$  is the number of memory representations and  $G$  is empirically set to 50 (ablation study in Fig. 4). After obtaining original temporal prototypes  $\hat{P}$ , we perform *knowledge retrieval* via only aggregating semantic-related memory from the bank:

$$P' = \sum_{g=1}^G \text{topk}(\hat{P}, m_g)m_g, \quad (3)$$

where  $\text{topk}$  is the function that retrieves  $O$  most similar prototypes from the bank according to the semantic correspondences. We take a hyper-parameter  $\kappa = O/G$  to determine the number of retrieved memory representations.  $P'$  is retrieved historical knowledge related to current task, which could be used to further enhance task-specific video representations.

**Knowledge Aggregation.** Knowledge Aggregation aims to make use of learned historical knowledge to enhance temporal features. Specifically, we first deliver the union of original temporal prototypes  $\hat{P}$  and retrieved memory  $P'$  by element-wise addition to obtain task-specific prototypes  $\tilde{P}$ . Then, support features  $\tilde{F}_s$  aggregate temporal knowledge provided by prototypes  $\tilde{P}$  via cross-attention mechanism:

$$\tilde{F}_s = \text{CrossAttn}(\tilde{F}_s, \tilde{P}), \quad (4)$$

where  $\text{CrossAttn}$  is the standard cross-attention operation, and  $\tilde{F}_s$  is enhanced temporal features of  $\tilde{F}_s$  by exploring inter-task relationships. By aggregating temporal knowledge from previous tasks, we strengthen discriminative dynamic patterns for each new episodic task.

**Knowledge Bank Updating.** At each episodic task, the temporal knowledge bank is continually updated to involve new learned knowledge from the current task. Our updating strategy is as follows: given  $i$ -th temporal prototype  $p_i$  in  $\hat{P}$ , if the knowledge bank is not full, the prototype is directly assigned; if the bank is full, we first compute the cosine similarity between current prototype and  $G$  memory representations in  $M$ , and update the most similar one as follows:

$$m_t = \text{SelectMax} \left( \frac{p_i \cdot m_j}{\|p_i\| \|m_j\|} \right), m_j \in M, \quad (5)$$

$$m_t \leftarrow \mu m_t + (1 - \mu) p_i, \quad (6)$$

where  $\text{SelectMax}$  denote the function that selects most similar memory representation from  $M$  as  $m_t$ , and  $\mu \in [0, 1]$  is the momentum for memory evolution. Note that during the testing phase, the temporal knowledge bank remains unchanged and does not store any information from testing data, avoiding information leakage.

**More In-Depth Discussion.** We emphasize that our designed Inter-task Knowledge Transfer (IKT) module strictly adheres to the standard few-shot learning protocol, and no information leakage occurs during testing. Specifically, the temporal knowledge bank in IKT only stores learned knowledge from support samples of training tasks and remains fixed during the testing phase. When performing knowledge retrieval at test time, our approach only accesses the support and query videos of the current task, and the knowledge bank used at test time remains unchanged and does *not* incorporate any features from test-time videos (*i.e.*, unseen classes).

In addition, our method learns useful temporal knowledge by capturing generalizable and task-shared semantic patterns during training, rather than introducing class-specific feature leakage from testing data. This is aligned with the goal of few-shot learning, which is to generalize to new classes by utilizing prior knowledge.

### 3.5 Training and Testing with HR<sup>2</sup>G-shot

**Training Objective.** After jointly exploring three types of relation modeling, we obtain support features  $\tilde{F}_s$  and query features  $\tilde{F}_q$ . Given  $i$ -th support frame-level features  $\tilde{f}_s^i \in \mathbb{R}^{T \times C}$  in  $\tilde{F}_s$  and  $j$ -th query frame-level features  $\tilde{f}_q^j \in \mathbb{R}^{T \times C}$  in  $\tilde{F}_q$ , like in previous

methods [3, 45], we adopt the “temporal alignment metric to obtain query-support distances:

$$\mathcal{D} = \text{Metric}(\tilde{f}_q^j, \tilde{f}_s^i), \quad (7)$$

where  $\text{Metric}$  denotes the OTAM [3] metric by default. Then we can use the output support-query distances as logits to compute cross-entropy loss  $\mathcal{L}_{\text{CE}}$  over the ground-truth labels.

**Testing.** During testing, We freeze the entire framework, and directly extracts support and query features in a single feedforward pass for the unseen test classes. Note that the temporal knowledge bank is also frozen, not incorporating any features from test-time videos. Finally, we can utilize the obtained distance in Eq. 7 as logits to produce query predictions.

## 4 EXPERIMENTS

### 4.1 Experimental Setup

**Dataset.** We evaluate our HR<sup>2</sup>G-shot on five commonly used datasets, *i.e.*, Kinetics [6], SSv2-small [14], SSv2-full [14], HMDB51 [22], and UCF101 [35]. For HMDB51 and UCF101, we adopt the few-shot split from [2, 63], with 31/10/10 classes and 70/10/21 classes for train/val/test, respectively. Following previous works [5, 46, 54], we divide Kinetics, SSv2-small and SSv2-full into three splits: 64/12/24 classes used for train, val, and test, respectively. The difference between SSv2-small and SSv2-full is that SSv2-full contains more videos per class in train set.

**Evaluation.** Following standard evaluation protocols [3, 26, 46, 57, 62], 5-way 1-shot and 5-shot accuracy over 10,000 tasks are used for evaluation.

### 4.2 Implementation Details

**Network Architecture.** HR<sup>2</sup>G-shot adopts pre-trained CLIP ViT-B [31] as our backbone for parameter-efficient fine-tuning, for a fair comparison with previous methods [30, 45, 55]. In IKT, we empirically set the size of temporal knowledge bank  $G = 40$  (see Fig. 4). By default, the number of temporal prototypes  $M$  is set to 3 (see Table 4c). For other hyper-parameters, we empirically set retrieval ratio  $\kappa$  and momentum  $\mu$  are to 0.8 (see Table 4b) and 0.99 (see Table 4d), respectively.

**Network Training.** In line with previous works [3, 19, 45, 57], we uniformly and sparsely sample  $T = 8$  frames from each video to encode frame-level representations. During the training phase, random horizontal flipping and color jitter are adopted for data augmentation. We freeze both the CLIP visual encoder and text encoder, and only finetune lightweight adapters in the visual encoder as [55]. We conducted training using the Adam [21] optimizer with the multi-step scheduler. Due to limited space, more implementation details are left in the appendix.

**Reproducibility.** All experiments are conducted on three NVIDIA 3090 GPUs with 24GB memory in PyTorch. To ensure reproducibility, full code will be released.

### 4.3 Comparison with State-of-the-Arts

Table 1 illustrates our compelling results over the top-leading FSAR solutions on five datasets (*i.e.*, SSv2-small [14], SSv2-full [14], HMDB51 [22], UCF101 [35], and Kinetics [6]). Our method reports the results on CLIP-ViT-B visual encoder. For spatial-related

**Table 1: Quantitative results on SSv2-small [14], SSv2-full [14], HMDB51 [22], UCF101 [35], and Kinetics [6] (see §4.3). “INet-RN50” denotes ResNet-50 pre-trained on ImageNet. The best results are highlighted.**

Method	Reference	Pre-training	SSv2-small		SSv2-full		HMDB51		UCF101		Kinetics	
			1-shot	5-shot	1-shot	5-shot	1-shot	5-shot	1-shot	5-shot	1-shot	5-shot
CMN [69]	ECCV’18	INet-RN50	34.4	43.8	36.2	48.9	-	-	-	-	60.5	78.9
OTAM [3]	CVPR’20	INet-RN50	-	-	42.8	52.3	-	-	-	-	73.0	85.8
AmeFuNet [13]	MM’20	INet-RN50	-	-	-	-	60.2	75.5	85.1	95.5	74.1	86.8
TRX [28]	CVPR’21	INet-RN50	-	59.1	-	64.6	-	75.6	-	96.1	63.6	85.9
TA <sup>2</sup> N [25]	AAAI’22	INet-RN50	-	-	47.6	61.0	59.7	73.9	81.9	95.1	72.8	85.8
MTFAN [52]	CVPR’22	INet-RN50	-	-	45.7	60.4	59.0	74.6	84.8	95.1	74.6	87.4
HyRSM [47]	CVPR’22	INet-RN50	40.6	56.1	54.3	69.0	60.3	76.0	83.9	94.7	73.7	86.1
STRM [40]	CVPR’22	INet-RN50	37.1	55.3	43.1	68.1	52.3	77.3	80.5	96.9	62.9	86.7
HCL [66]	ECCV’22	INet-RN50	38.9	55.4	47.3	64.9	59.1	76.3	82.6	94.5	73.7	85.8
MoLo [46]	CVPR’23	INet-RN50	41.9	56.2	55.0	69.6	60.8	77.4	86.0	95.5	74.0	85.6
GgHM [57]	ICCV’23	INet-RN50	-	-	54.5	69.2	85.2	96.3	61.2	76.9	74.9	87.4
CLIP-FSAR [45]	IJCV’24	CLIP-RN50	52.0	55.8	58.1	62.8	69.2	80.3	91.3	97.0	87.6	91.9
CLIP-Freeze [31]	ICML’21	CLIP-ViT-B	29.5	42.5	30.0	42.4	58.2	77.0	89.7	95.7	78.9	91.9
CapFSAR [49]	Arxiv’23	CLIP-ViT-B	45.9	59.9	51.9	68.2	65.2	78.6	93.3	97.8	84.9	93.1
MVP-shot [30]	Arxiv’24	CLIP-ViT-B	55.4	62.0	-	-	77.0	88.1	96.8	99.0	91.0	95.1
MA-FSAR [55]	Arxiv’24	CLIP-ViT-B	59.1	64.5	63.3	72.3	83.4	87.9	97.2	99.2	95.7	96.0
CLIP-FSAR [45]	IJCV’24	CLIP-ViT-B	54.6	61.8	62.1	72.1	77.1	87.7	97.0	99.1	94.8	95.4
<b>HR<sup>2</sup>G-shot (ours)</b>	-	CLIP-ViT-B	<b>60.2</b>	<b>66.0</b>	<b>65.4</b>	<b>74.8</b>	<b>85.6</b>	<b>88.6</b>	<b>98.0</b>	<b>99.3</b>	<b>95.2</b>	<b>96.4</b>

**Table 2: The impact and parameters of core components on SSv2-small [14] and HMDB51 [22] under the 5-way 1-shot setting (see §4.4).**

Method Component	Model Params	SSv2-small	HMDB51
BASELINE	71.0M	55.0	81.2
ISC <i>only</i>	73.2M (+2.2)	58.7	84.0
IKT <i>only</i>	74.5M (+3.5)	57.8	83.2
<b>HR<sup>2</sup>G-shot (Ours)</b>	<b>76.7M (+5.7)</b>	<b>60.2</b>	<b>85.6</b>

**Table 3: Ablations of different inter-video interaction manner in ISC on SSv2-small [14] and HMDB51 [22] under the 5-way 1-shot setting (see §4.4).**

Method	FLOPs (M)	SSv2-small	HMDB51
Video-level global attention	53	56.5	83.6
Frame-level dense attention	252	58.9	84.2
<b>Ours</b>	<b>58</b>	<b>60.2</b>	<b>85.6</b>

datasets, our method yields remarkable performance on most task settings across HMDB51, UCF101, and Kinetics. Especially for 1-shot tasks, it surpasses the previous SOTA (*i.e.*, MA-FSAR [55]) by 2.2% on HMDB51 and 0.8% on UCF101, respectively. Temporal-related datasets (SSv2-small and SSv2-full) require models to comprehend complex temporal information, making it much more challenging. Our approach still achieves dominant results on SSv2-small and SSv2-full, surpassing other competitors across all metric task settings. This reinforces our belief that our method makes use of the temporal knowledge bank, which collects temporal cues from historical tasks, to yield discriminative temporal features. All of the above improvements across all datasets and task settings show our HR<sup>2</sup>G-shot has strong generalization for different scenes. We attribute this to the fact that we learn task-specific temporal features by transferring knowledge at both video-level and task-level.

## 4.4 Diagnostic Experiment

**Key Component Analysis.** We first investigate the effectiveness of each component in HR<sup>2</sup>G-shot, *i.e.*, Inter-video Semantic Correlation (ISC) and Inter-task Knowledge Transfer (IKT), which is summarized in Table 2. First, our proposed ISC leads to 3.7% and 2.8% performance gains against the baseline on SSv2-small [14] and HMDB51 [22], respectively, demonstrating the value of inter-video relation modeling. Second, after incorporating our proposed IKT into the baseline, our method improves on the two datasets by 2.8% and 2.0%, verifying that capturing task-shared temporal knowledge by exploring inter-task relationships can yield task-specific video representations. Third, our full model HR<sup>2</sup>G-shot achieves the best performance, confirming the joint effectiveness of our overall algorithm design. Different from reported learnable model parameters in Table 5, we provide full model parameters in Table 2. As seen, our algorithm brings a modest amount of extra parameters, while leveraging such a performance leap.

**Impact of Inter-video Interaction Manner in ISC.** We study the impact of our fine-grained inter-video interaction (Eq. 1) by contrasting it with video-level global attention [47] and frame-level dense attention. “video-level global attention” refers to conducting inter-video interaction via global video features, and “frame-level dense attention” means one frame token interacts with all other frame tokens in current task. As outlined in Table 3, our fine-grained inter-video interaction proves to be *effective*—it outperforms video-level global attention and frame-level dense attention by 3.7% and 1.3% on SSv2-small respectively, and *efficient*—its FLOPs are significantly less than frame-level dense attention. The reason why our fine-grained interaction outperforms frame-level dense attention may be that frame-level dense attention often introduces redundant or noisy interactions. Thus, we conclude that our fine-grained

**Table 4: A set of ablation studies on SSv2-small [14] and HMDB51 [22] under the 5-way 1-shot setting (§4.4). The adopted network designs are marked in red.**

Method	SSv2-small	HMDB51
support-support	58.7	84.7
query-support	59.0	84.5
full	57.8	84.0
<b>Ours</b>	<b>60.2</b>	<b>85.6</b>

(a) Masked Interaction Strategy

Retrieval ratio $\kappa$	SSv2-small	HMDB51
$\kappa = 0.3$	58.9	84.3
$\kappa = 0.5$	59.5	84.9
<b><math>\kappa = 0.7</math></b>	<b>60.2</b>	<b>85.6</b>
$\kappa = 0.9$	59.9	85.3
$\kappa = 1.0$	59.7	85.2

(b) Retrieval Ratio

Prototype Number $M$	SSv2-small	HMDB51
$M = 1$	59.0	84.7
$M = 2$	59.5	85.0
<b><math>M = 3</math></b>	<b>60.2</b>	<b>85.6</b>
$M = 4$	59.6	85.3
$M = 8$	58.8	85.2

(c) Prototype Number

Momentum Coefficient $\mu$	SSv2-small	HMDB51
$\mu = 0$	57.2	83.1
$\mu = 0.5$	59.0	84.4
$\mu = 0.9$	59.4	85.0
<b><math>\mu = 0.99</math></b>	<b>60.2</b>	<b>85.6</b>
$\mu = 0.999$	59.9	85.4

(d) Momentum Coefficient

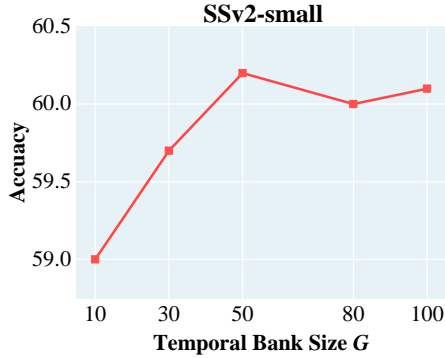


**Figure 4: The impact of temporal bank size  $G$  in IKT on SSv2-small [14] under the 5-way 1-shot setting (§4.4).**

inter-video interaction achieves a trade-off between effectiveness and efficiency for capturing task-specific temporal cues.

**Impact of Different Masked Interaction Strategies in ISC.** We further analyze the influence of our masked interaction strategy on SSv2-small [14] and HMDB51 [22]. Fig. 3(b)(c)(d) shows three other alternative masked strategies, *i.e.*, support-support interaction, query-support interaction and full interaction. As reported in Table 4a, our masked interaction strategy (*i.e.*, adaptive Intraction Mask) yields significant performance advancements compared with other alternatives. This suggests that designing proper masked interactions by respecting the difference between support and query videos contributes to better fine-grained cross-video interactions.

**Impact of Different Retrieval Ratio  $\kappa$  in IKT.** We next investigate the impact of retrieval ratio  $\kappa$  (Eq. 3), which controls the number of retrieved memory representations from the knowledge bank. Table 4b provides comparison results with regard to different retrieval ratios under the 1-shot setting on SSv2-small [14] and HMDB51 [22]. We can clearly observe that, our algorithm performs best with a relatively large retrieval ratio (*i.e.*,  $\kappa = 0.7$ ) on SSv2-small. This verifies that we discard the semantic-unrelated temporal knowledge in the bank to alleviate the negative effects of meaningless semantic information. When  $\kappa$  is too small, the performance

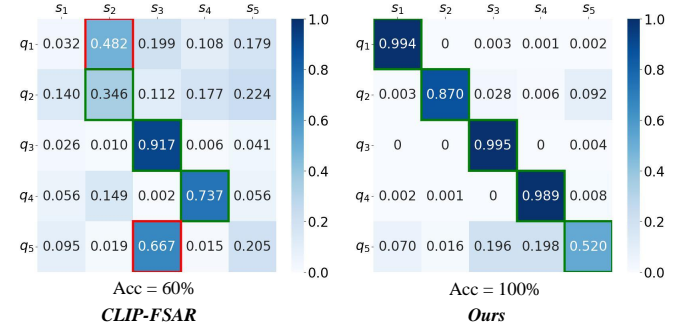


**Figure 5: Similarity visualization between query samples ( $q_n$ ) and support prototypes ( $s_n$ ) with different methods in a meta-test episode from HMDB51 [22] (see §4.5). A higher score indicates a greater degree of similarity. The green box indicates correct prediction and the red box indicates incorrect prediction.**

degrades. We speculate this is because our algorithm discards too many useful memory representations related to the current task.

**Impact of Temporal Prototype Number  $M$  in IKT.** Table 4c reports the performance of our HR<sup>2</sup>G-shot with regard to the number of temporal prototypes.  $M=1$  means that directly treating one video as a global representation. For  $M=8$ , we maintain original frame-level features as temporal prototypes. After constructing learnable prototypes to summarize discriminative temporal representations, we observe consistent improvements. For example, our HR<sup>2</sup>G-shot gains the best performance (*i.e.*, 60.2% accuracy on SSv2-small dataset) when  $M=3$ .

**Impact of Momentum Coefficient  $\mu$  in IKT.** We probes the impact of momentum coefficient  $\mu$  (Eq.6) on SSv2-small [14] and HMDB51 [22] in Table 4d. We can clearly observe that, our algorithm performs better with a relatively large coefficient (*i.e.*,  $\mu = 0.99$ ), but not too large (*i.e.*,  $\mu = 0.999$ ). When  $\mu$  is too small, the performance decreases. In particular, at the extreme of no momentum (*i.e.*,  $\mu = 0$ ), the performance significantly degrades.

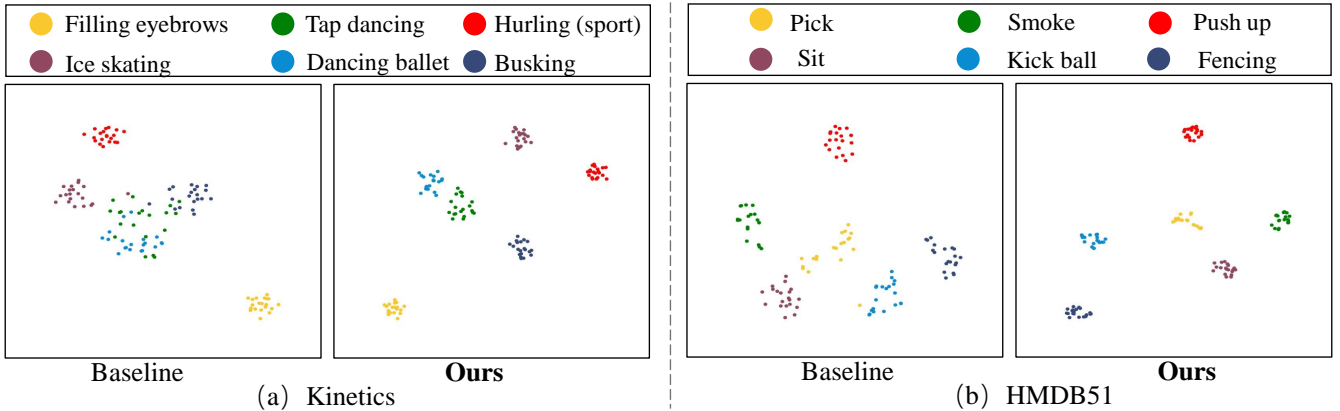


Figure 6: T-SNE feature visualization of six classes learned by baseline and HR<sup>2</sup>G-shot on Kinetics [6] and HMDB51 [22] (§4.5).

Table 5: Complexity analysis for 5-way 1-shot HMDB51 [22] and SSv2-small [14] evaluation. Note that there are 1 query samples per class. Here, we report trainable parameters, GPU memory, and Speed for each model. “Acc<sup>1</sup>” and “Acc<sup>2</sup>” are the accuracy on HMDB51 and SSv2-small, respectively (§4.4).

Method	Params	Memory	Speed	Acc <sup>1</sup>	Acc <sup>2</sup>
CLIP-FSAR	89.5M	14.2G	36.7ms	77.1	54.6
HR <sup>2</sup> G-shot(ours)	19.9M	14.3G	39.9ms	85.6	60.2

**Impact of Bank Size  $G$  in IKT.** Then we study the influence of our knowledge bank in Fig. 4. As seen from Fig. 4, our algorithm HR<sup>2</sup>G-shot gains stable improvements (*i.e.*, 59.0%→60.2%) on SSv2-small [14] as the bank size grows (*i.e.*,  $G = 50$ ). This demonstrates that i) there indeed exist some task-shared temporal patterns in the bank, and ii) making use of these task-shared temporal patterns can ensuring a sufficient temporal understanding for each task. However, further increasing  $G$  cause marginal returns in performance. Thus, we set bank size  $G$  to 50 to achieve a better trade-off between accuracy and computation costs.

**Efficiency Analysis.** To analyze the effectiveness of our HR<sup>2</sup>G-shot, we list comparison results with CLIP-FSAR [45] in terms of trainable parameters, GPU memory, and inference speed in Table 5. We choose ViT-B as our visual encoder. Note that different from full model parameters in Table 2, Table 5 reports trainable parameter comparison. As shown in Table 5, compared to CLIP-FSAR, our method introduces fewer trainable parameters. Though efficient in terms of parameters, our algorithm brings slight inference delay and memory costs. However, the hierarchical relation modeling allows our method to outperform CLIP-FSAR in terms of classification accuracy, *i.e.*, 8.5% and 5.6% accuracy improvements on HMDB51 [22] and SSv2-small [14] over CLIP-FSAR, respectively.

## 4.5 Quality Analysis

**Similarity visualization.** To qualitatively demonstrate the effectiveness of hierarchical relation modeling in our HR<sup>2</sup>G-shot, we visualize the predicted similarities between query and support prototypes with different approaches (*i.e.*, CLIP-FSAR [45] and ours) for one task of HMDB51 in Fig. 5. As seen, our HR<sup>2</sup>G-shot can

Table 6: Generalization performance of our method with different temporal alignment metrics on SSv2-small [14] and HMDB51 [22] under the 5-way 1-shot setting (§4.6).

Temporal Metric	SSv2-small	HMDB51
CLIP-FSAR (Bi-MHM)	54.1	77.0
<b>Ours (Bi-MHM)</b>	<b>60.1</b>	<b>85.0</b>
CLIP-FSAR (TRX)	53.8	77.4
<b>Ours (TRX)</b>	<b>60.4</b>	<b>85.7</b>
CLIP-FSAR (OTAM)	54.6	77.1
<b>Ours (OTAM)</b>	<b>60.2</b>	<b>85.6</b>

make more accurate decisions for similar classes in each task compared with CLIP-FSAR. Specifically, for the first query sample in Fig. 5, the incorrect decision obtained by CLIP-FSAR can be rectified by jointly modeling three types of relations. These results further demonstrate that our method can capture task-specific temporal cues via transferring knowledge at both video-level and task-level. **The visualization of Feature Distribution.** Fig. 6 visualizes learned features of baseline and our algorithm HR<sup>2</sup>G-shot with ISC and IKT via the t-SNE tool. We clearly observe that after conducting inter-video and inter-task interactions, learned video features become more compact (intra-class) and better separated (inter-class). As shown in Fig. 6(b), the three classes “Smoke”, “Sit”, and “Pick” become clearly distinguishable from each other after conducting hierarchical relation modeling. The above phenomena suggest that we can gain task-specific temporal features by transferring knowledge at both video-level and task-level, ensuring better feature discrimination. See more examples in Appendix.

## 4.6 Generalization Study

To demonstrate that HR<sup>2</sup>G-shot generalizes well to different alignment metrics, Table 6 report comparison results on HMDB51 [22] and SSv2-small [14] with regard to different temporal metrics (*cf.* Eq. 7). Different temporal metrics are adopted, including OTAM [3], TRX [28] and Bi-MHM [47]. As seen, our HR<sup>2</sup>G-shot consistently achieves better performance compared with CLIP-FSAR [45], regardless of the temporal alignment metric employed. This shows that our method can adapt to any temporal alignment metric.



## 5 CONCLUSION

In this work, we present HR<sup>2</sup>-G-shot, a novel Hierarchical Relation-augmented Representation Generalization framework for FSAR, which captures task-specific temporal cues from multiple perspectives (*i.e.*, inter-frame, inter-video, and inter-task). Rather than only conducting inter-frame temporal interactions, we further **i)** perform fine-grained cross-video temporal interaction for exploring inter-video relationships, and **ii)** aggregate useful temporal knowledge from previous tasks for learning inter-task relationships. Our framework is hierarchical, elegant, and gains outstanding performance on five standard FSAR datasets, *i.e.*, SSv2-full, SSv2-small, HMDB51, UCF101, and Kinetics. Our work offers a fresh perspective to current FSAR solutions by hierarchically exploring multi-level relations, and we wish it to inspire future research in this field.

## REFERENCES

- [1] Alon Albalak, Colin A Raffel, and William Yang Wang. 2024. Improving few-shot generalization by exploring and exploiting auxiliary data. In *NeurIPS*, Vol. 36.
- [2] Mina Bishay, Georgios Zoumpourlis, and Ioannis Patras. 2019. Tarn: Temporal attentive relation network for few-shot and zero-shot action recognition. In *BMVC*.
- [3] Kaidi Cao, Jingwei Ji, Zhangjie Cao, Chien-Yi Chang, and Juan Carlos Niebles. 2020. Few-shot video classification via temporal alignment. In *CVPR*. 10618–10627.
- [4] Meiqi Cao, Xiangbo Shu, Jiachao Zhang, Rui Yan, Zechao Li, and Jinhui Tang. 2024. EventCrab: Harnessing Frame and Point Synergy for Event-based Action Recognition and Beyond. *arXiv preprint arXiv:2411.18328* (2024).
- [5] Yichao Cao, Xiu Su, Qingfei Tang, Shan You, Xiaobo Lu, and Chang Xu. 2022. Searching for Better Spatio-temporal Alignment in Few-Shot Action Recognition. *NeurIPS* 35 (2022), 21429–21441.
- [6] Joao Carreira and Andrew Zisserman. 2017. Quo vadis, action recognition? a new model and the kinetics dataset. In *CVPR*. 6299–6308.
- [7] Zitian Chen, Yanwei Fu, Yu-Xiong Wang, Lin Ma, Wei Liu, and Martial Hebert. 2019. Image deformation meta-networks for one-shot learning. In *CVPR*. 8680–8689.
- [8] Zitian Chen, Yanwei Fu, Yinda Zhang, Yu-Gang Jiang, Xiangyang Xue, and Leonid Sigal. 2019. Multi-level semantic feature augmentation for one-shot learning. *IEEE Transactions on Image Processing* 28, 9 (2019), 4594–4605.
- [9] Hao Cheng, Siyuan Yang, Joey Tianyi Zhou, Lanqing Guo, and Bihan Wen. 2023. Frequency guidance matters in few-shot learning. In *ICCV*. 11814–11824.
- [10] Li Fei-Fei, Robert Fergus, and Pietro Perona. 2006. One-shot learning of object categories. *IEEE Transactions on Pattern Analysis and Machine Intelligence* 28, 4 (2006), 594–611.
- [11] Christoph Feichtenhofer, Haoqi Fan, Jitendra Malik, and Kaiming He. 2019. Slow-fast networks for video recognition. In *ICCV*. 6202–6211.
- [12] Chelsea Finn, Pieter Abbeel, and Sergey Levine. 2017. Model-agnostic meta-learning for fast adaptation of deep networks. In *ICML*. 1126–1135.
- [13] Yuqian Fu, Li Zhang, Junke Wang, Yanwei Fu, and Yu-Gang Jiang. 2020. Depth guided adaptive meta-fusion network for few-shot video recognition. In *ACM MM*. 1142–1151.
- [14] Raghav Goyal, Samira Ebrahimi Kahou, Vincent Michalski, Joanna Materzynska, Susanne Westphal, Heuna Kim, Valentin Haebel, Ingo Fruend, Peter Yanilos, Moritz Mueller-Freitag, et al. 2017. The "something something" video database for learning and evaluating visual common sense. In *ICCV*. 5842–5850.
- [15] Peng Huang, Xiangbo Shu, Rui Yan, Zhewei Tu, and Jinhui Tang. 2024. Appearance-Agnostic Representation Learning for Compositional Action Recognition. *IEEE Transactions on Circuits and Systems for Video Technology* (2024).
- [16] Peng Huang, Rui Yan, Xiangbo Shu, Zhewei Tu, Guangzhao Dai, and Jinhui Tang. 2023. Semantic-Disentangled Transformer With Noun-Verb Embedding for Compositional Action Recognition. *IEEE Transactions on Image Processing* (2023).
- [17] Wenbo Huang, Jinghui Zhang, Xuwei Qian, Zhen Wu, Meng Wang, and Lei Zhang. 2024. SOAP: Enhancing Spatio-Temporal Relation and Motion Information Capturing for Few-Shot Action Recognition. In *ACM MM*. 4572–4580.
- [18] Yifei Huang, Lijin Yang, Guo Chen, Hongjie Zhang, Feng Lu, and Yoichi Sato. 2024. Matching Compound Prototypes for Few-Shot Action Recognition. *International Journal of Computer Vision* (2024), 1–26.
- [19] Yifei Huang, Lijin Yang, and Yoichi Sato. 2022. Compound prototype matching for few-shot action recognition. In *ECCV*. 351–368.
- [20] Muhammad Abdullah Jamal and Guo-Jun Qi. 2019. Task agnostic meta-learning for few-shot learning. In *CVPR*. 11719–11727.
- [21] Diederik P Kingma and Jimmy Ba. 2014. Adam: A method for stochastic optimization. *arXiv preprint arXiv:1412.6980* (2014).
- [22] Hildegard Kuehne, Hueihan Jhuang, Estibaliz Garrote, Tomaso Poggio, and Thomas Serre. 2011. HMDB: a large video database for human motion recognition. In *ICCV*. 2556–2563.
- [23] Chengjian Li, Xiangbo Shu, Qiongjie Cui, Yazhou Yao, and Jinhui Tang. 2024. FTMoMamba: Motion Generation with Frequency and Text State Space Models. *arXiv preprint arXiv:2411.17532* (2024).
- [24] Kai Li, Yulun Zhang, Kungpeng Li, and Yun Fu. 2020. Adversarial feature hallucination networks for few-shot learning. In *CVPR*. 13470–13479.
- [25] Shuyuan Li, Huabin Liu, Rui Qian, Yuxi Li, John See, Mengjuan Fei, Xiaoyuan Yu, and Weiyao Lin. 2022. TA2N: Two-stage action alignment network for few-shot action recognition. In *AAAI*, Vol. 36. 1404–1411.
- [26] Baolong Liu, Tianyi Zheng, Peng Zheng, Daizong Liu, Xiaoye Qu, Junyu Gao, Jianfeng Dong, and Xun Wang. 2023. Lite-MKD: A Multi-modal Knowledge Distillation Framework for Lightweight Few-shot Action Recognition. In *ACM MM*. 7283–7294.
- [27] Huabin Liu, Weixian Lv, John See, and Weiyao Lin. 2022. Task-adaptive spatial-temporal video sampler for few-shot action recognition. In *ACM MM*. 6230–6240.
- [28] Toby Perrett, Alessandro Masullo, Tilo Burghardt, Majid Mirmehdi, and Dima Damen. 2021. Temporal-relational crosstransformers for few-shot action recognition. In *CVPR*. 475–484.
- [29] Hongyu Qu, Jianan Wei, Xiangbo Shu, and Wenguan Wang. 2025. Learning Clustering-based Prototypes for Compositional Zero-shot Learning. *arXiv preprint arXiv:2502.06501* (2025).
- [30] Hongyu Qu, Rui Yan, Xiangbo Shu, Hailiang Gao, Peng Huang, and Guo-Sen Xie. 2024. MVP-Shot: Multi-Velocity Progressive-Alignment Framework for Few-Shot Action Recognition. *arXiv preprint arXiv:2405.02077* (2024).
- [31] Alec Radford, Jong Wook Kim, Chris Hallacy, Aditya Ramesh, Gabriel Goh, Sandhini Agarwal, Girish Sastry, Amanda Askell, Pamela Mishkin, Jack Clark, et al. 2021. Learning transferable visual models from natural language supervision. In *ICML*. 8748–8763.
- [32] Aravind Rajeswaran, Chelsea Finn, Sham M Kakade, and Sergey Levine. 2019. Meta-learning with implicit gradients. In *NeurIPS*, Vol. 32.
- [33] Andrei A Rusu, Dushyant Rao, Jakub Sygnowski, Oriol Vinyals, Razvan Pascanu, Simon Osindero, and Raia Hadsell. 2019. Meta-learning with latent embedding optimization. In *ICLR*.
- [34] Jake Snell, Kevin Swersky, and Richard Zemel. 2017. Prototypical networks for few-shot learning. In *NeurIPS*, Vol. 30.
- [35] Khurram Soomro, Amir Roshan Zamir, and Mubarak Shah. 2012. UCF101: A dataset of 101 human actions classes from videos in the wild. *arXiv preprint arXiv:1212.0402* (2012).
- [36] Siyuan Sun and Hongyang Gao. 2024. Meta-AdaM: An meta-learned adaptive optimizer with momentum for few-shot learning. In *NeurIPS*, Vol. 36.
- [37] Flood Sung, Yongxin Yang, Li Zhang, Tao Xiang, Philip HS Torr, and Timothy M Hospedales. 2018. Learning to compare: Relation network for few-shot learning. In *CVPR*. 1199–1208.
- [38] Hao Tang, Jun Liu, Shuanglin Yan, Rui Yan, Zechao Li, and Jinhui Tang. 2023. M3Net: Multi-view Encoding, Matching, and Fusion for Few-shot Fine-grained Action Recognition. In *ACM MM*. 1719–1728.
- [39] Yutao Tang, Benjamin Béjar, and René Vidal. 2024. Semantic-aware Video Representation for Few-shot Action Recognition. In *WACV*. 6458–6468.
- [40] Anirudh Thatipelli, Sanath Narayan, Salman Khan, Rao Muhammad Anwer, Fahad Shahbaz Khan, and Bernard Ghanem. 2022. Spatio-temporal relation modeling for few-shot action recognition. In *CVPR*. 19958–19967.
- [41] Oriol Vinyals, Charles Blundell, Timothy Lillicrap, Daan Wierstra, et al. 2016. Matching networks for one shot learning. In *NeurIPS*, Vol. 29.
- [42] Limin Wang, Zhan Tong, Bin Ji, and Gangshan Wu. 2021. Tdn: Temporal difference networks for efficient action recognition. In *CVPR*. 1895–1904.
- [43] Xiao Wang, Yan Yan, Hai-Miao Hu, Bo Li, and Hanzhi Wang. 2024. Cross-Modal Contrastive Learning Network for Few-Shot Action Recognition. *IEEE Transactions on Image Processing* (2024).
- [44] Xiao Wang, Weirong Ye, Zhongang Qi, Xun Zhao, Guangge Wang, Ying Shan, and Hanzhi Wang. 2021. Semantic-guided relation propagation network for few-shot action recognition. In *ACM MM*. 816–825.
- [45] Xiang Wang, Shiwei Zhang, Jun Cen, Changxin Gao, Yingya Zhang, Deli Zhao, and Nong Sang. 2024. CLIP-guided prototype modulating for few-shot action recognition. *International Journal of Computer Vision* 132, 6 (2024), 1899–1912.
- [46] Xiang Wang, Shiwei Zhang, Zhiwu Qing, Changxin Gao, Yingya Zhang, Deli Zhao, and Nong Sang. 2023. MoLo: Motion-augmented Long-short Contrastive Learning for Few-shot Action Recognition. In *CVPR*. 18011–18021.
- [47] Xiang Wang, Shiwei Zhang, Zhiwu Qing, Zhengrong Zuo, Changxin Gao, Rong Jin, and Nong Sang. 2022. Hybrid relation guided set matching for few-shot action recognition. In *CVPR*. 19948–19957.
- [48] Xiang Wang, Shiwei Zhang, Zhiwu Qing, Zhengrong Zuo, Changxin Gao, Rong Jin, and Nong Sang. 2024. HyRSM++: Hybrid relation guided temporal set matching for few-shot action recognition. *Pattern Recognition* 147 (2024), 110110.

- [49] Xiang Wang, Shiwei Zhang, Hangjie Yuan, Yingya Zhang, Changxin Gao, Deli Zhao, and Nong Sang. 2023. Few-shot Action Recognition with Captioning Foundation Models. *arXiv preprint arXiv:2310.10125* (2023).
- [50] Yuyang Wanyan, Xiaoshan Yang, Chaofan Chen, and Changsheng Xu. 2023. Active exploration of multimodal complementarity for few-shot action recognition. In *CVPR*. 6492–6502.
- [51] Cong Wu, Xiao-Jun Wu, Linze Li, Tianyang Xu, Zhenhua Feng, and Josef Kittler. 2024. Efficient Few-Shot Action Recognition via Multi-level Post-reasoning. In *ECCV*. 38–56.
- [52] Jiamin Wu, Tianzhu Zhang, Zhe Zhang, Feng Wu, and Yongdong Zhang. 2022. Motion-modulated temporal fragment alignment network for few-shot action recognition. In *CVPR*. 9151–9160.
- [53] Zhirong Wu, Yuanjun Xiong, Stella X Yu, and Dahua Lin. 2018. Unsupervised feature learning via non-parametric instance discrimination. In *CVPR*. 3733–3742.
- [54] Haifeng Xia, Kai Li, Martin Renqiang Min, and Zhengming Ding. 2023. Few-shot video classification via representation fusion and promotion learning. In *ICCV*. 19311–19320.
- [55] Jiazheng Xing, Mengmeng Wang, Xiaojun Hou, Guang Dai, Jingdong Wang, and Yong Liu. 2024. Multimodal adaptation of clip for few-shot action recognition. *arXiv preprint arXiv:2308.01532* (2024).
- [56] Jiazheng Xing, Mengmeng Wang, Yong Liu, and Boyu Mu. 2023. Revisiting the Spatial and Temporal Modeling for Few-shot Action Recognition. In *AAAI*, Vol. 37. 3001–3009.
- [57] Jiazheng Xing, Mengmeng Wang, Yudi Ruan, Bofan Chen, Yaowei Guo, Boyu Mu, Guang Dai, Jingdong Wang, and Yong Liu. 2023. Boosting Few-shot Action Recognition with Graph-guided Hybrid Matching. In *ICCV*. 1740–1750.
- [58] Zhen Xing, Qi Dai, Han Hu, Jingjing Chen, Zuxuan Wu, and Yu-Gang Jiang. 2023. Svformer: Semi-supervised video transformer for action recognition. In *CVPR*. 18816–18826.
- [59] Taojiannan Yang, Yi Zhu, Yusheng Xie, Aston Zhang, Chen Chen, and Mu Li. 2023. AIM: Adapting Image Models for Efficient Video Action Recognition. In *ICLR*.
- [60] Xu Yang, Huaxiu Yao, and Ying Wei. 2024. One Meta-tuned Transformer is What You Need for Few-shot Learning. In *ICML*.
- [61] Sung Whan Yoon, Jun Seo, and Jaekyun Moon. 2019. Tapnet: Neural network augmented with task-adaptive projection for few-shot learning. In *ICML*. 7115–7123.
- [62] Tianwei Yu, Peng Chen, Yuanjie Dang, Ruohong Huan, and Ronghua Liang. 2023. Multi-speed global contextual subspace matching for few-shot action recognition. In *ACM MM*. 2344–2352.
- [63] Hongguang Zhang, Li Zhang, Xiaojuan Qi, Hongdong Li, Philip HS Torr, and Piotr Koniusz. 2020. Few-shot action recognition with permutation-invariant attention. In *ECCV*. 525–542.
- [64] Ruixiang Zhang, Tong Che, Zoubin Ghahramani, Yoshua Bengio, and Yangqiu Song. 2018. Metagan: An adversarial approach to few-shot learning. In *NeurIPS*, Vol. 31.
- [65] Yilun Zhang, Yuqian Fu, Xingjun Ma, Lizhe Qi, Jingjing Chen, Zuxuan Wu, and Yu-Gang Jiang. 2023. On the Importance of Spatial Relations for Few-shot Action Recognition. In *ACM MM*. 2243–2251.
- [66] Sipeng Zheng, Shizhe Chen, and Qin Jin. 2022. Few-shot action recognition with hierarchical matching and contrastive learning. In *ECCV*. 297–313.
- [67] Tianfei Zhou, Meijie Zhang, Fang Zhao, and Jianwu Li. 2022. Regional semantic contrast and aggregation for weakly supervised semantic segmentation. In *CVPR*. 4299–4309.
- [68] Hao Zhu and Piotr Koniusz. 2023. Transductive few-shot learning with prototype-based label propagation by iterative graph refinement. In *CVPR*. 23996–24006.
- [69] Linchao Zhu and Yi Yang. 2018. Compound memory networks for few-shot video classification. In *ECCV*. 751–766.
- [70] Linchao Zhu and Yi Yang. 2020. Label independent memory for semi-supervised few-shot video classification. *IEEE Transactions on Pattern Analysis and Machine Intelligence* 44, 1 (2020), 273–285.